Different Modes of Crack Propagation in Burning Solid Propellants

K. K. Kuo,* J. Moreci,† and J. Mantzaras†
The Pennsylvania State University, University Park, Pennsylvania

The motivation for this research came from the lack of proper understanding of propagation and branching processes in burning solid propellants. These processes are vital in defining safe operating conditions of high energy solid propellants and interpreting important phenomena during the initial phase of deflagration-to-detonation transition (DDT). Several experiments have been conducted, and propellant samples have been recovered by rapid pressurization followed by depressurization. For different pressurization rates, four major modes of crack propagation and/or branching are observed. For very low $\partial p/\partial t$, burning occurs without crack propagation. For $\partial p/\partial t$ in the order of 1.4 to 15 GPa/s, an existing crack propagates along its initial direction as a single crack (propagation mode). At high pressurization rates of 30 GPa/s or higher, multiple branching in various directions is observed (branched mode); and at intermediate $\partial p/\partial t$, single crack propagation is accompanied by local branching (mixed mode). The amount of surface area generated by mixed or branched modes is substantially higher than that of the single crack propagation mode, and in real motors, could cause sufficiently severe burning in the damaged zone to result in rocket motor failure.

I. Introduction

CRACKS may exist in solid propellant grains as a result of manufacturing defects, aging, or mechanical damage. In the combustion of these damaged grains, the propagation and branching of cracks may significantly increase the burning surface area in the grain, thus, initiating chamber overpressure and possible rocket motor failure. In seriously damaged grains, these processes could also increase the chance of deflagration-to-detonation transition (DDT). It is the aim of this research to gain deeper understanding of the crack propagation process by experimentally examining modes of damage corresponding to various operating conditions.

The specific objectives of the investigation are 1) to create damage in propellant samples with prefabricated flaws by rapid pressure loading and combustion; 2) to study the degree of damage produced in the propellant by interrupting the combustion process and recovering the samples before they are consumed; and 3) to reveal the major modes of crack propagation and/or branching by characterizing the damage under various pressurization rates.

II. Method of Approach

Many variables govern the processes of crack propagation and branching. These include the initial pressurization rate, propellant type, sample geometry, initial temperature, etc. The initial pressurization rate is considered to be the most dominant parameter. The testing philosophy adopted for this research is to vary the initial pressurization rate while holding other parameters constant. The propellant type under investigation is an AP/HTPB (73/27) composite with an average oxidizer size of 200 μm.

Presented as Paper 85-1176 at AIAA/SAE/ASME/ASEE 21st Joint Propulsion Conference, Monterey, CA, July 8-10, 1985; received Nov. 5, 1985; revision received March 14, 1985.

*Distinguished Alumni Professor. Associate Fellow AIAA.
†Graduate Assistant.

Experimental Setup

In order to generate damage in propellant samples under different initial pressurization rates and, to subsequently recover the samples for examination, a modified version of the experimental setup used in previous studies[1-6] is employed. Major components of the test setup are 1) a crack propagation test chamber to house the sample; 2) a driving motor to create high-pressure and high-temperature gases; 3) a depressurization chamber, which causes dynamic extinction of the sample after a desired time interval; 4) a nitrogen injection system which cools the sample and inner surfaces of the test chamber; and 5) a timing control circuit which coordinates the event. A schematic diagram of the test rig and control circuit is shown in Fig. 1.

The crack propagation test chamber is designed to withstand high pressures, while allowing observation and pressure history recording of the propellant sample as it is damaged. The two-dimensional sample includes a triangular cavity with a 3-mm-long slit at the tip and an outer taper angle of 3 deg (see Fig. 2a). The prefabricated slit (Fig. 2b), is cut by a sharp razor blade to simulate a crack of zero thickness. The triangular opening of the propellant sample facilitates pressure loading on the slanted surfaces and is not part of the initial crack tip contour. The outer taper angle simulates confinement conditions that a propellant grain may encounter in a rocket motor.

The sample is installed in the main chamber and held in position by three brass holders. To seal the propellant in the chamber and provide a viewing port for the event, a plexiglass window and window retainer are bolted into place over the sample. As shown in Fig. 3, there are two window openings in the retainer. The reason for having two view openings instead of one is to avoid window buckling and retainer plate distortion when the chamber is pressurized. The circular port is used to observe combustion product gases as they enter the test chamber from the driving motor. Crack propagation and/or branching can be observed through the rectangular port.

When the main igniter is activated, the propellant sample is pressurized by high-pressure, high-temperature gases. These gases penetrate into the crack cavity causing ignition, pressurization, mechanical deformation, and crack propagation and/or branching. The mass and type of charge in the main igniter determines the pressurization rate the sample encounters and, consequently, the mode of crack propagation.

To recover the propellant sample the following procedure is used. When the pressure in the main chamber reaches a prescribed value, the timing control circuit activates primer no. 2 located in the depressurization chamber assembly (see Fig. 1). The product gases from the gas generator pressurize the free space between the two bursting diaphragms, causing them to rupture after a short delay. Rapid depressurization of the main chamber follows. The timing control circuit then activates primer no. 3 located in the nitrogen injection system. The product gases from this generator drive the flying pin through the N_2 injection system diaphragm, allowing immediate introduction of low temperature nitrogen into the main chamber for quenching. The time interval between activating primers nos. 2 and 3 is preselected. The fast change in chamber operating conditions leads the system to dynamic extinction[7] and allows the sample to be recovered. Settings on the timing circuit device determine the peak chamber pressure and depressurization rate.

In some experiments, in order to achieve extremely rapid pressurization rates followed by dynamic extinction, the depressurization chamber and exit nozzle are replaced by a number of thin brass bursting diaphragms mounted directly on the main chamber. The added area provided by removing the exit nozzle is helpful in causing sufficiently rapid depressurization for dynamic extinction. The peak chamber pressure and depressurization rate are controlled in this case by the strength of the bursting diaphragms.

The data acquisition system consists of two major parts: a pressure recording system and an event filming system. Pressure measurements are made using five piezoelectric transducers mounted on the main chamber against the rear surface of the propellant at the following locations (see Fig. 1): crack cavity entrance (G1), initial crack tip region (G2), center of the sample beyond the initial crack tip (G3), lower cavity (G4), and upper cavity (G5). Pressure signals from the transducers are amplified by charge amplifiers and captured by a transient waveform recorder. A high-speed 16-mm motion picture camera capable of a framing rate of 44,000 pictures/s is used to film the event through the observation ports of the window retainer.

III. Experimental Results

Depending upon the initial pressurization rate, four distinct modes of structural damage (modes A, B, C, and D) at the tip region were observed. The first, mode A, corresponds to very low $\partial p/\partial t$ (much less than 1 GPa/s) and involves no mechanical damage. The displacement of the crack tip is due solely to recession of the propellant surface by burning. Under this condition, an existing crack will not cause any departure from normal operating conditions. The upper limit of the pressurization rate for this mode depends upon propellant formulation, confinement state, and initial conditions. Since this represents the normal or trivial case of crack propagation, no specific investigation into this area was conducted at this time.

A representative set of data, including some pressure-time traces, film records, and recovered sample photographs for modes B, C, and D with a detailed description of the observed phenomena is given below.

Mode B: Single Crack Propagation

At low pressurization rates, as measured at the entrance of the crack cavity (of the order of 1.4–15 GPa/s), single crack propagation was observed. The *p-t* traces recorded at the entrance (G1), crack tip (G2), center region (G3), and the end regions of the sample (G4 and G5) are shown in Fig. 4. The film record of this test firing is shown in Fig. 5 with detailed interpretations given in Table 1. The dark zones in these pictures are due to the obstruction by the steel window retainer

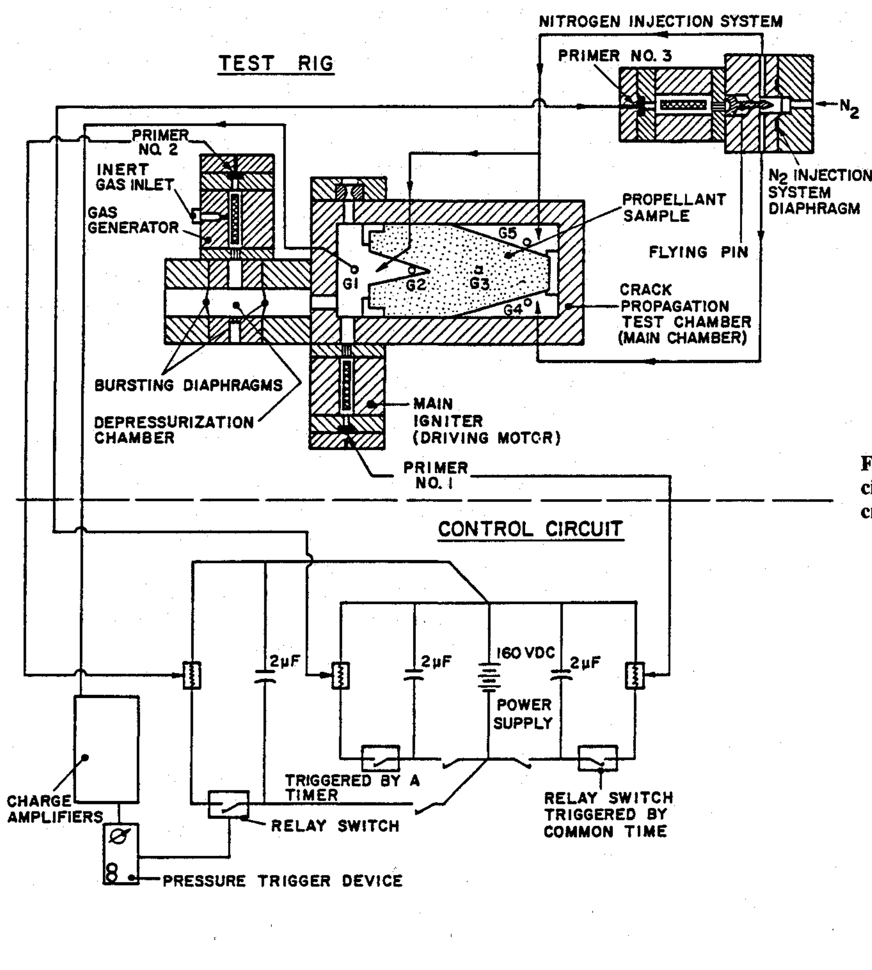

Fig. 1 Schematic diagram of the test rig and control circuit for recovery of propellant samples during crack propagation and/or branching.

Table 1 Film interpretation of single crack propagation (test firing no. DNICP-22)

Picture	Time, μs	Observations and interpretations
		a) Initial phase of crack propagation
1	0	Hot igniter gas enters into triangular crack cavity.
2–7	55–330	Typical opening mode crack propagation, with crack tip moving in axial direction. Triangular shape of luminous region near crack tip verifies existence of single crack. Slopes of crack cavity walls show distinct breaks.
8–13	385–660	Opening of crack increases. Cavity walls become flat as slope breaks disappear.
14–15	717–770	Crack walls are spreading apart, especially near the tip region. The walls become parallel.
16–21	825–1000	Hot gases start to penetrate into interface between sample and plexiglass retainer. Crack tip does not bifurcate, but continues to propagate in its original direction.
22–25	1155–1320	Burning area in crack region increases in size while maintaining same shape. Bright lines parallel to sample axis beyond crack cavity are caused by flame penetration between sample and plexiglass window.
26–260	1375–14,245	Hot gas penetration increases to the point where observation of the propellant sample is not possible.
		b) Second phase of crack propagation
261–304	14,300–16,665	Propellant sample is under quick depressurization, but the burning is essentially sustained. The single extended crack is clearly visible in center of picture. Bright region beyond crack is caused by continued flame penetration between sample and window.
		c) Extinction phase
305–317	16,720–17,380	Luminosity of region beyond tip is decreasing rapidly, while propellant contours remain highly visible.
318–322	17,435–17,655	Most of the combustion gases have escaped through the exit ports. Sample is barely visible before extinction.

Table 2 Film interpretation of multiple crack propagation and branching (test firing no. DNICP-28)

Picture	Time, μs	Observations and interpretations
		a) Initial phase of crack propagation and branching
1–6	0–330	Hot gas penetration into triangular crack cavity.
7–10	396–594	Initiation of crack growth (propagation).
11	660	Tendency for bifurcation (initiation of crack branching).
12–24	726–1518	Severe burning is evident in damaged region where crack has split into two major branches. The left branch further splits into several smaller subbranches while it continues to propagate.
		As a result of the enormous amount of local gas generation, high-pressure gradients exist between burned and unburned zones. This causes luminous gases to flow beyond the crack front and into the space between sample and window.
		Penetrating combustion gases in the side cavity are less luminous. Mushroomed region flattens out and becomes less visible on the edge, due to heat loss and, possibly, closing of gap between window and propellant. The left side of sample burns severely and causes more damage to the propellant.
		b) Extinction phase
25–62	1650–4026	Flame penetrated region between sample and plexiglass window diminishes, thus, enhancing visibility of crack tip location.
63–100	4092–6534	The luminous region decreases as depressurization of the chamber continues.

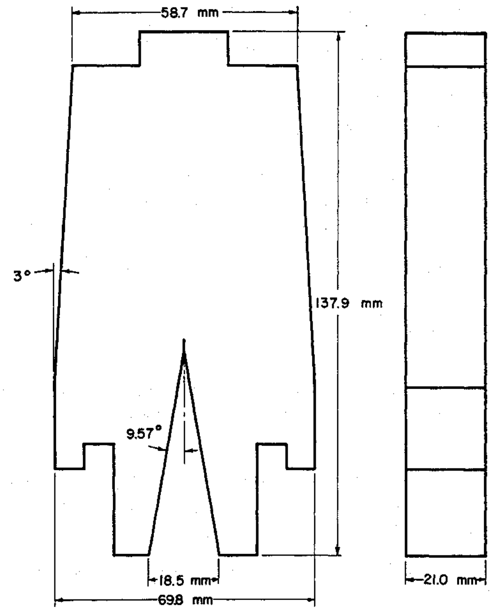

Fig. 2a Geometry of propellant crack sample used in propagation and branching experiments.

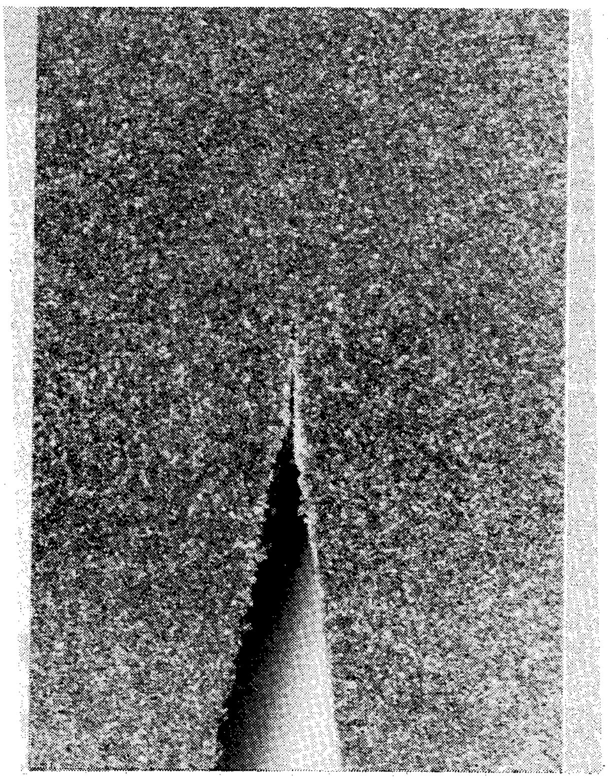

Fig. 2b Close-up view of sample crack tip and cavity.

material between the circular port and rectangular window (see Fig. 3). Pressures at the crack entrance and tip increase almost linearly, then decay monotonically after the bursting diaphragms rupture. The peak pressure and pressurization rate at the crack tip (G2) are higher than at other locations. This indicates that the burning at the crack tip introduces local gas accumulation and damage. However, since the area generated by single crack propagation is limited, it causes no significant pressurization in regions beyond the crack tip, as revealed by the nearly flat *p-t* traces at locations G3–G5.

Examination of the recovered sample reveals that under these conditions the existing crack is extended in the direction of its initial configuration, as shown in Fig. 6. The

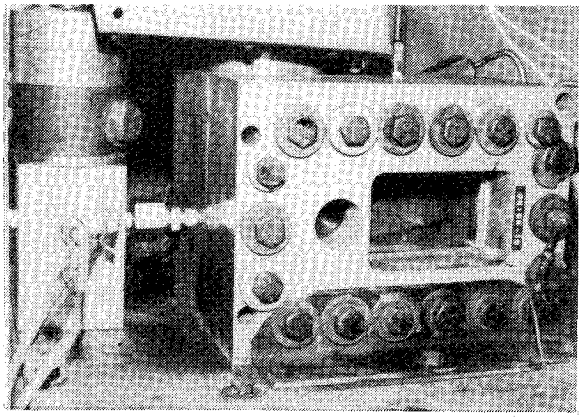

Fig. 3 Front view of the main chamber and depressurization chamber used in crack propagation and branching studies.

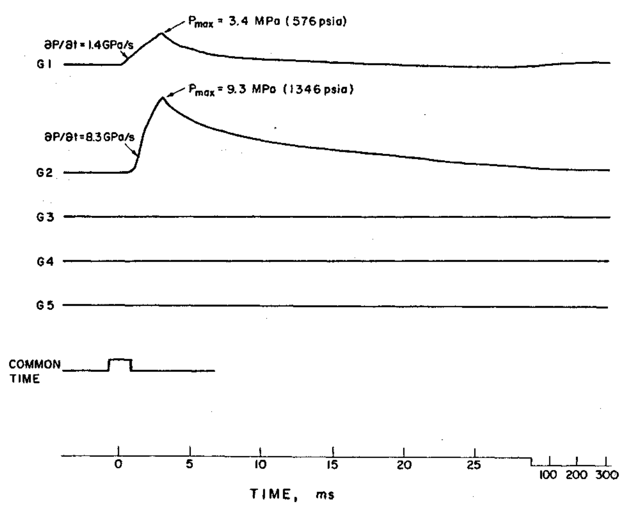

Fig. 4 Pressure-time traces of single crack propagation (test firing DNICP-22).

characteristic nature of mode B is such that the damage generated by the loading is restricted to the crack boundary and does not greatly affect the overall integrity of the propellant. The generated crack void fraction is small and does not significantly increase the overall burning surface area (as evidenced by Figs. 4 and 5).

Mode C: Crack Propagation with Branching

At intermediate pressurization rates, single crack propagation can be initiated and followed by local branching at various axial locations (see Figs. 7a and 7b). The damage generated in mode C is much more extensive than that of mode B. Figure 8 shows a number of interesting portions of the film event. Detailed interpretation of these film clips is presented in Table 2. The recovered propellant sample surface and crack cavity legs are marked by numerous erosion ditches. A side view of one of the legs of a sample crack surface sample is shown in Fig. 9. The surface roughness is believed to be the result of the high-pressure, high-temperature gases produced near the crack tip region. These gases erode the propellant surface and legs as they exit the high pressure zone. Based upon visual comparison between various recovered samples, the total specific surface area created in mode C is clearly higher than that of mode B.

Mode D: Crack Branching

Mode D crack branching involves the development of multiple cracks originating from a central point. Crack branches emanate from this common point and propagate in

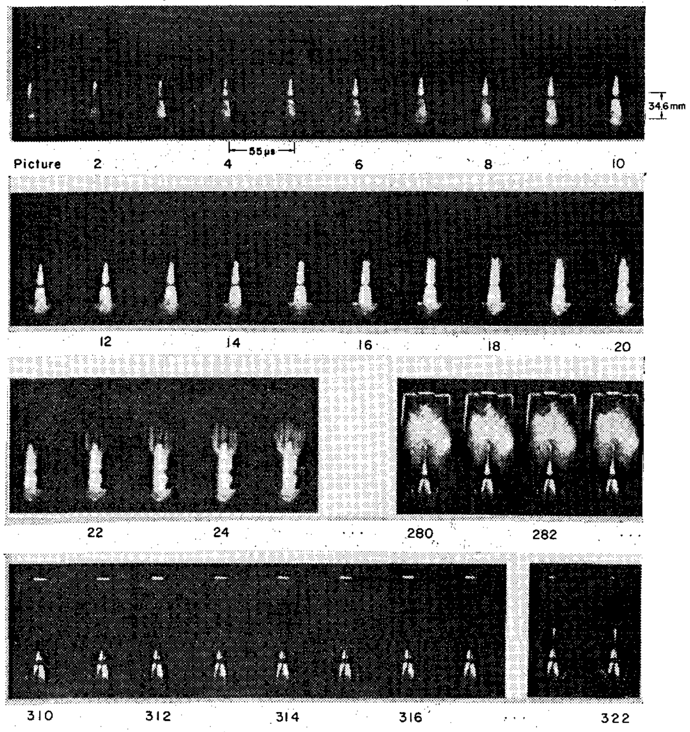

Fig. 5 Film record of single crack propagation (test firing DNICP-22).

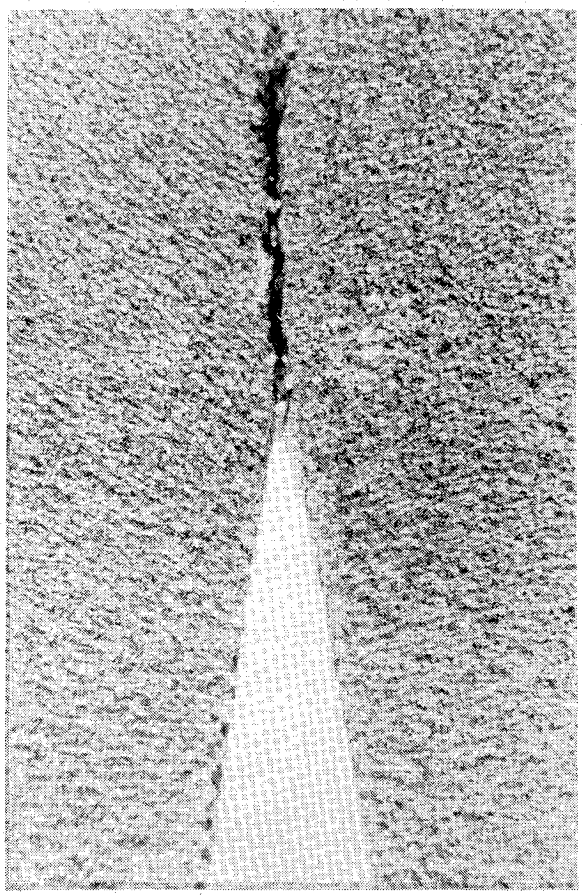

Fig. 6 Recovered sample exhibiting mode B crack propagation (same magnification as Fig. 2b).

Fig. 7a Front view of recovered sample exhibiting mode C crack propagation and branching (same magnification as Fig. 2b).

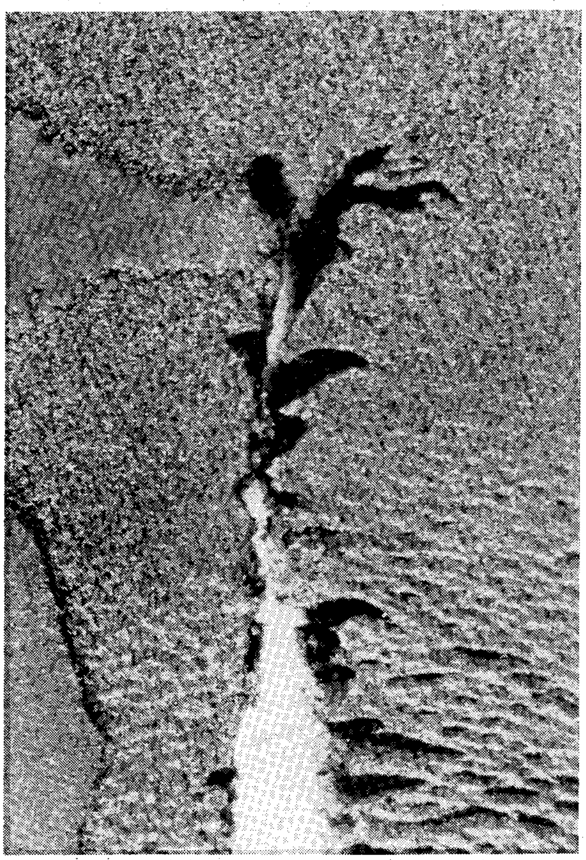

Fig. 7b Rear view of sample in Fig. 7a.

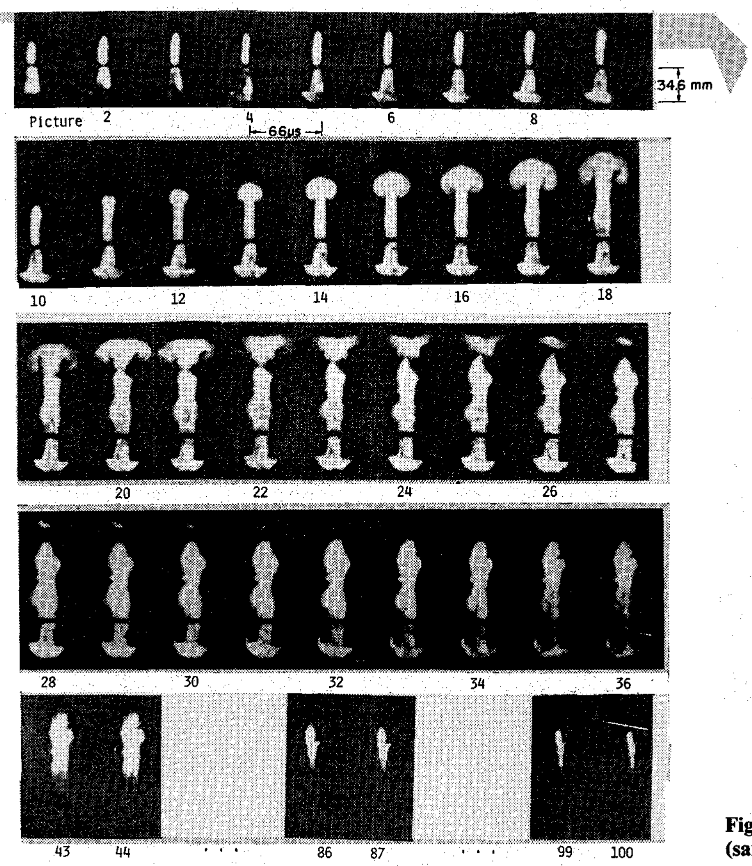

Fig. 8 Film record of mode C crack propagation and branching (test firing DNICP-28).

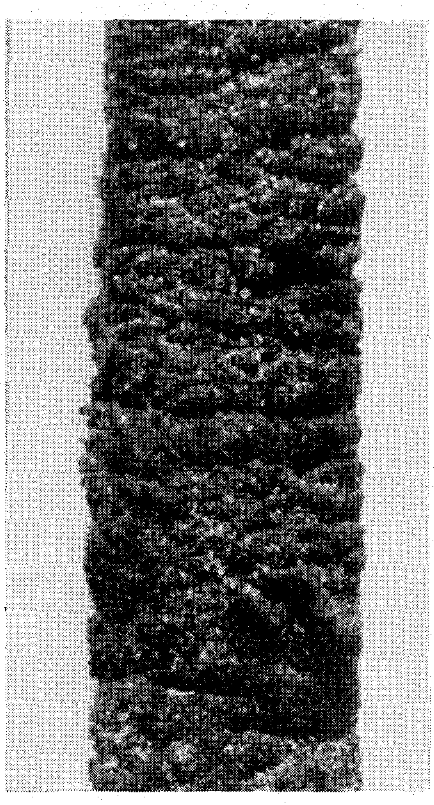

Fig. 9 Erosion ditches formed in mode D sample legs by high gasification rates (the front view of the propellant surface facing the initial triangular cavity).

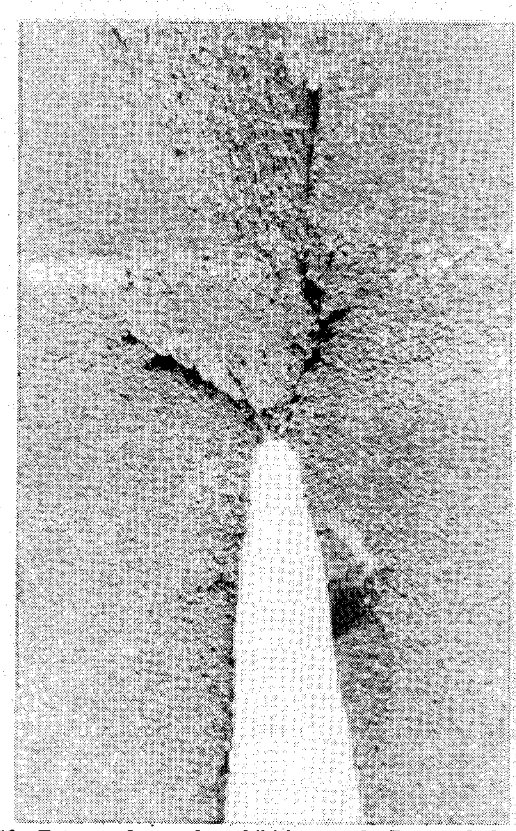

Fig. 10 Recovered sample exhibiting mode D_1 crack branching (same magnification as Fig. 2b).

different directions. This mode can be subdivided into two groups (mode D_1 and D_2), depending upon the number of major crack branches. Mode D_1 is associated with fewer branches, sometimes only two, where it may be called bifurcation (see Fig. 10). Mode D_2 is associated with numerous branches (see Fig. 11). The *p-t* traces in Fig. 12, which are representative of mode D branching, correspond to a very high pressurization rate (42 GPa/s) at the crack cavity entrance. In this case, the recovered sample shown in Fig. 10 reveals that the existing crack branches and propagates into several macrocracks. The high initial gas loading rate generates strong pressure waves which oscillate within the crack cavity and throughout the propellant sample. As a result of the large increase in specific burning area generated from crack branching at the tip, the pressure history at the center of the sample (G3) is substantially different from the previous case shown in Fig. 4. The *p-t* trace at G3 shows that the sample in the damaged zone sensed significant pressure loading caused by the partial burning and flame penetration in this region.

Film records of test firings with branched mode D_1 or D_2 show rapid changes in crack contours, followed by flame penetration between the propellant samples and the sacrificial windows. The flame penetration is caused by steep pressure gradients which exist between the burned and unburned regions. These film records are omitted in this paper; more detailed information is available in Ref. 2. Comparison of recovered mode D_1 and D_2 samples (Figs. 10 and 11) with those of mode B (see Fig. 6) reveals an area of much greater damage near the crack tip. Multiple branching and cracking in numerous directions are observed. The generation of multiple cracks at very high pressurization rates is due mostly to the simultaneous attainment of critical stress for fracture at numerous points in the same central area. Following the creation of flow channels, high pressure gases penetrate the local void regions and cause additional damage along the crack branches. This is fundamentally different from the

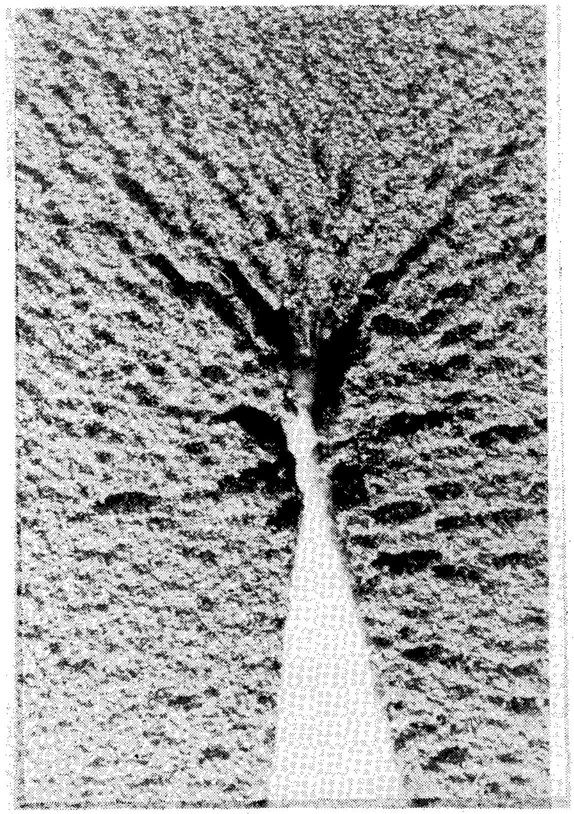

Fig. 11 Recovered sample exhibiting mode D_2 crack branching (same magnification as Fig. 2b).

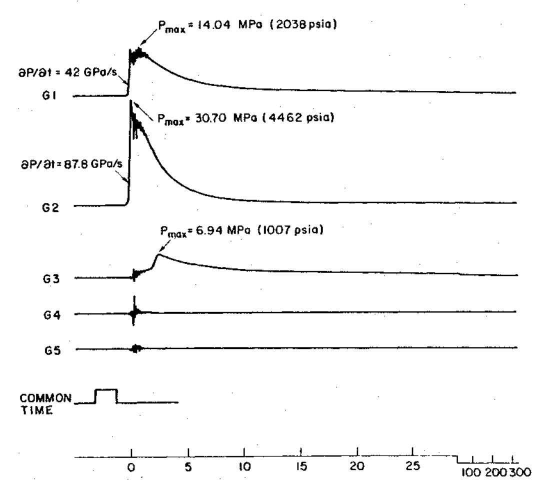

Fig. 12 Pressure-time traces of mode D crack branching (test firing DNICP-27).

opening mode of a single crack propagation which takes place via a relatively slow splitting action.

IV. Summary and Conclusions

Many damaged propellant samples were recovered from test firings at different pressurization rates. Four different modes of damage were observed. Depending upon the initial pressurization rate, the mechanical damage of the sample adjacent to the crack tip region differs significantly. The first mode (mode A) involves no mechanical damage. Under this condition, an existing crack will not cause any departure from normal motor operating characteristics. The second mode (mode B), which occurs at relatively low pressurization rates (1.4–15 GPa/s), creates local damage restricted to single crack propagation. Such single crack propagation, if continued over a period of time, may cause motor case burn through or other undesirable burning conditions.

The third and fourth modes (modes C and D) were observed at intermediate and high pressurization rates, respectively. These modes involve crack propagation and multiple branching of the tip region in various directions, generating either small or large amounts of void fractions. Due to the existence of high-pressure gradients, the high-temperature gases driven from the high-pressure burning zone cause significant erosion of the propellant sample, especially on the surface. These modes can also produce high degrees of damage due to the strong interaction between the burning and fracture processes. It is apparent that the combustion/fracture coupled mechanism creates a large specific surface area for burning; therefore, a real rocket motor may be highly susceptible to failure under these conditions. This problem deserves great attention in the future, especially in view of the recent tragedy of the Challenger Space Shuttle flight caused by the malfunction of one of its solid rocket boosters.

Acknowledgment

This research has been sponsored by the Power Program of the Office of Naval Research, Arlington, VA, under Contract N000014-79-C-0762. Dr. Richard S. Miller served as the technical monitor and program manager for this contract. His support of this research is greatly appreciated. Thanks are also due to Prof. Richard A. Schapery of Texas A&M University for a useful exchange of ideas in crack propagation studies.

References

[1]Kuo, K. K., Siefert, J. G., Mantzaras, J., Hsieh, W. H., and Koo, F. H., "Nitramine Propellent Crack Tip Ignition and Crack Propagation of a Burning Sample Under Rapid Pressurization," Annual Report, Office of Naval Research, Oct. 1983.

[2]Kuo, K. K., Mantzaras, J., Koo, F. H., Kim, J. U., and Moreci, J., "Crack Propagation and Branching in Burning Solid Propellants and Ignition of Nitramine-Based Composite Propellants Under Rapid Pressurization," Annual Report, Office of Naval Research, Dec. 1984.

[3]Mantzaras, J., Andiroglu, E., and Kuo, K. K., "Recovery of Damaged Solid Propellants by Interrupting Burning and Crack Propagation Processes," *Proceedings of 1984 JANNAF Propulsion Systems Hazards Meeting,* Aberdeen Proving Ground, MD, June 1984.

[4]Kuo, K. K., Siefert, J. G., Kumar, M., Hsieh, W. H., and Andiroglu, E., "Mechanism of Crack Propagation in Burning Solid Propellants," *Proceedings of 1983 JANNAF Propulsion Systems Hazards Meeting,* CPIA Pub. 381, July 1983, pp. 125–138.

[5]Siefert, J. G., and Kuo, K. K., "Crack Propagation in Burning Solid Propellants," *AIAA Progress Series,* Vol. 94, edited by J. R. Bowen, N. Manson, A. K. Oppenheim, and R. I. Soloukhin, 1985, pp. 575–595.

[6]Kuo, K. K., et al., "Propellant Crack Tip Ignition and Propagation Under Rapid Pressurization," Summary Report, Office of Naval Research, Power Program, Oct. 1982.

[7]DeLuca, L., "Extinction Theories and Experiments," *AIAA Progress Series,* Vol. 90, edited by K. K. Kuo and M. Summerfield, 1984.